IEEE Access
Multidisciplinary | Rapid Review | Open Access Journal

Received September 22, 2019, accepted October 11, 2019, date of publication November 6, 2019,
date of current version January 6, 2020.

Digital Object Identifier 10.1109/ACCESS.2019.2951940

Effects of Residual Hardware Impairments on Secure NOMA-Based Cooperative Systems

MEILING LI[1], BASSANT SELIM[2], (Member, IEEE), SAMI MUHAIDAT[3], (Senior Member, IEEE), PASCHALIS C. SOFOTASIOS[3,4], (Senior Member, IEEE), MEHRDAD DIANATI[5], (Senior Member, IEEE), PAUL D. YOO[6], (Senior Member, IEEE), JIE LIANG[7], (Senior Member, IEEE), AND ANHONG WANG[1]

[1]School of Electronics Information Engineering, Taiyuan University of Science and Technology, Taiyuan 030024, China
[2]Electrical Engineering Department, ETS, University of Quebec, Montreal, QC H3C 1K3, Canada
[3]Center for Cyber-Physical Systems, Department of Electrical Engineering and Computer Science, Khalifa University, Abu Dhabi 127788, UAE
[4]Department of Electrical Engineering, Tampere University, 33101 Tampere, Finland
[5]Wireless Manufacturing Group, University of UK, Coventry CV4 7AL, U.K.
[6]Department of Computer Science and Information Systems, Birkbeck College, University of London, London WC1E 7HX, U.K.
[7]School of Engineering Science, Simon Fraser University, Burnaby, BC V5A 1S6, Canada

Corresponding author: Sami Muhaidat (muhaidat@ieee.org)

This work was supported in part by the National Natural Science Foundation of China under Grant 61672373 and Grant 51504255, in part by the Key Research and Development Program of Shanxi under Grant 201903D121117, in part by the Scientific and Technological Innovation Programs of Higher Education Institutions in Shanxi under Grant 201802090, in part by the Program of One hundred Talented People of Shanxi Province, in part by the Scientific and Technology Innovation Program of Shanxi Province under Grant 201705D131025, in part by the Project of Collaborative Innovation Center of Internet+3D Printing in Shanxi Province, in part by the Key Innovation Team of the 1331 Project of Shanxi Province, and in part by the Khalifa University of Science and Technology under Grant KU/RC1-C2PS-T2/8474000137 and Grant KU/FSU-8474000122.

ABSTRACT Non-orthogonal multiple access (NOMA) has been proposed as a promising technology that is capable of improving the spectral efficiency of fifth-generation wireless networks and beyond. However, in practical communication scenarios, transceiver architectures inevitably suffer from radio frequency (RF) front-end related impairments that cause non-negligible performance degradation. This issue can be addressed by analog and digital signal processing algorithms, however, inevitable aspects of this approach such as time-varying hardware characteristics and imperfect compensation schemes result to detrimental residual distortions. In the present contribution we investigate the physical layer security of NOMA-based amplify-and-forward relay systems under such realistically incurred residual hardware impairment (RHI) effects. Exact and asymptotic analytic expressions for the corresponding outage probability (OP) and intercept probability (IP) of the considered setup over multipath fading channels are derived and corroborated by respective simulation results. Based on this, it is shown that RHI affects both the legitimate users and eavesdroppers by increasing the OP and decreasing the IP. For a fixed OP, RHI generally increases the corresponding IP, thereby reducing the secure performance of the system. Further interesting insights are provided, verifying the importance of the offered results for the effective design and deployment of secure cooperative communication systems.

INDEX TERMS Intercept probability, non-orthogonal multiple access, outage probability, physical layer security, residual hardware impairments.

I. INTRODUCTION

The increasing number of connected devices and the continuously increasing quality of service (QoS) requirements pose several theoretical and technological challenges on the effective design and deployment of fifth-generation (5G) networks and beyond [1]. Some of the related stringent requirements are the substantially higher data rates, energy efficiency, low latency, and massive connectivity of diverse mobile devices. In this context, the current infrastructure and

The associate editor coordinating the review of this manuscript and approving it for publication was Zhu Han.

available methods for the design and deployment of wireless communication systems are limited and thus unable to support such highly demanding wireless systems and services.

Motivated by the above, non-orthogonal multiple access (NOMA) was recently introduced as a promising candidate for 5G systems, in an effort to overcome the aforementioned challenges. The key concept underlying NOMA is to utilize non-orthogonal resources such as the power or code domains for multiple access instead of the time or frequency domains used in orthogonal multiple access (OMA) schemes. In contrast to OMA, NOMA does not allocate orthogonal resources to the different users, instead successive interference cancellation (SIC) is performed. As a result, it provides better spectral efficiency, supports more connected devices, achieves reduced transmission latency, higher cell-edge throughput and relaxed channel feedback because only the received signal strength is required [2]–[4].

Cooperative diversity, mostly used in infrastructure-less networks, emerged in the past decade as a promising approach to increase the spectral and power efficiencies, broaden network coverage, and reduce the outage probability. NOMA based cooperative systems have been studied in an effort to improve the system performance. Examples include, a cooperative multi-user NOMA system using SIC, that exploits the knowledge of some users about other users' messages [5]; a NOMA-based cooperative half-duplex relaying system, that assumes Rayleigh fading channels [6]; and a cooperative relay system with space-time block-coded NOMA that is capable of achieving higher spectral efficiency [7]. Furthermore, a full-duplex relay NOMA system that can assist users with weak channel conditions was addressed under the realistic assumption of imperfect self-interference cancellation [8], [9]. In the same context, a relay selection strategy for a two-user NOMA scenario has also been proposed in [10], whereas downlink multi-user NOMA systems have been investigated for the case where an amplify and forward relay is used to assist the transmission [11], [12]. In this context, the corresponding outage probability and ergodic sum rate were investigated under Nakagami$-m$ distributed fading conditions.

It is also recalled that the uncertainty and time-varying nature of wireless channels can create a secure communication link without the need for encryption algorithms. In this regard, physical layer security has recently attracted considerable attention, particularly in the context of multiple access systems. In NOMA-based systems, the existing wireless communication link is vulnerable to eavesdropping due to the nature of broadcasting by the underlying power domain multiplexing. Hence, physical layer security technology can be used to achieve secure transmissions, as it has been widely addressed in OMA systems [13]–[16].

However, in NOMA based communication systems, physical layer security is associated with challenges that have been considered in many recent literature. For example, in [17] a related investigation of the robustness of NOMA against external eavesdroppers considered the secure outage probability under large-scale networks in the presence of artificial noise, which was assumed in order to improve the secrecy performance. Furthermore, the secrecy sum rate for all users has been analyzed over Rayleigh fading channels, assuming the transmitter (TX) has perfect knowledge of the channel state information (CSI) of the eavesdropper [18]. Other studies have considered the decoding order and transmission rates to optimize the power allocation in NOMA systems in the presence of an external eavesdropper [19], and analyzed the secure beamforming in a downlink multiple input single output (MISO) NOMA system by optimizing the power allocation [20]. A NOMA communication system has also been analyzed for the case where the TX conveys a confidential message to only one user, while keeping it secret from all the other users [21]. In the same context, a more recent study [22] considered one source, two destination users and one eavesdropper in the analysis of secure performance under different antenna selection schemes. In addition, in [23], assuming the decode-and-forward (DF) protocol, different relay selection schemes were investigated to improve the secure outage performance. In [24], the secrecy outage probability over Rayleigh fading channels was analyzed for a 2 users cooperative NOMA system, considering both the amplify-and-forward (AF) and DF protocols. Based on [24], the authors in [25] evaluated the secrecy outage probability over Nakagami-m fading channels by extending the wiretapping cases to the internal and external eavesdropping scenarios. Finally, the authors in [26], [27] considered a cooperative NOMA system where the near user acts as a relay to assist the transmission to the far user and both users' secrecy outage probability was analyzed.

Nevertheless, all aforementioned contributions assume an ideal RF front-end, which is not typically the case in realistic communication systems. Indeed, the continuously increasing demands placed on RF transceivers have led to challenging design targets including low cost, low power dissipation, and a small form factor. In this context, direct-conversion transceivers offer an effective RF front-end solution, because they demand neither external intermediate frequency filters nor image rejection filters. Such transceiver architectures are low cost and can be integrated on chips rather straightforwardly. However, they suffer from RF impairments which are considerably less severe in their bulky heterodyne counterparts [28]. Typical examples of such RF impairments include local oscillator phase noise, DC offsets, in-phase/quadrature-phase imbalance, and amplifier nonlinearities. It is recalled that the mitigation of RF impairments in communication systems can be achieved using analog and digital signal processing algorithms [28]–[30]. Yet, factors such as time-varying hardware characteristics and imperfect compensation schemes leave some residual distortion, known as residual hardware impairment (RHI), which can be accurately modeled as an additive noise to the transmitted/received signal [31].

Several works have investigated the impact of RHI on relay networks. For instance, the impact of hardware impairments

has been investigated in a massive MIMO full-duplex relaying system. There, the end-to-end achievable rate was derived under large scale antenna arrays, where the effect of hardware impairments was modeled by the transmitted and received distortion noise [32]. Other related studies have considered the effect of hardware impairments by deriving closed-form expressions for the outage probability and throughput for two-way multi-antenna and multi-relay amplify-and-forward networks [33], or by investigating the ergodic channel capacity of a dual-hop amplify-and-forward relay system [34]. The effect of hardware impairments at the source, relays, and destination nodes has been investigated in AF/DF multiple relay networks under Rician fading conditions [35]. Meanwhile, in the context of NOMA, recently a few works considering the impact of hardware impairments on NOMA systems have emerged such as [36] where the effects of common RF impairments on NOMA are highlighted. Likewise, the outage probability of both single-carrier and multi-carrier NOMA systems under the effects of in-phase/quadrature-phase imbalance was derived [37], whilst the outage probability of cooperative NOMA systems in the presence of RHI was determined in [38]–[40]. Further recently, the effects of RHI in the simultaneous wireless information and power transfer NOMA network was investigated in terms of outage probability in [41].

In spite of the detrimental effects of RHI on wireless communication systems, such effects are often neglected in the analysis of conventional and emerging communication systems, leading to idealistic results that deviate from those encountered in realistic communication scenarios. This is the case for the secrecy performance of cooperative multi-user NOMA systems. Motivated by this, the current analysis considers a practical system where the RF front-ends are affected by RHI and investigates its performance in a secure multi-user cooperative NOMA scenario. SpeciĭAcally, the contributions of this work are listed below:

- We quantify the secrecy outage performance of a cooperative multi-user NOMA system consisting of a base station, a relay, multiple users, and an eavesdropper, all suffering from RHI. Closed form analytical expressions are derived for the exact and asymptotic OP and IP under Rayleigh multipath fading conditions.
- We investigate how TX RHI only, receiver (RX) RHI only and joint TX/RX RHI at the source, relay, legitimate users, and eavesdropper, affect the secure performance of cooperative multi-user NOMA systems. This is realized in terms of the corresponding IP and OP for which, exact analytical expressions are derived for the above impairment scenarios.
- By introducing the main-to-eavesdropper ratio (MER), we derive the diversity order of the asymptotic OP in the high signal - noise - ratio (SNR) regime and the asymptotic IP in the high MER region. The trade-off between the outage and intercept probabilities is quantified, providing useful insights into the system's performance.

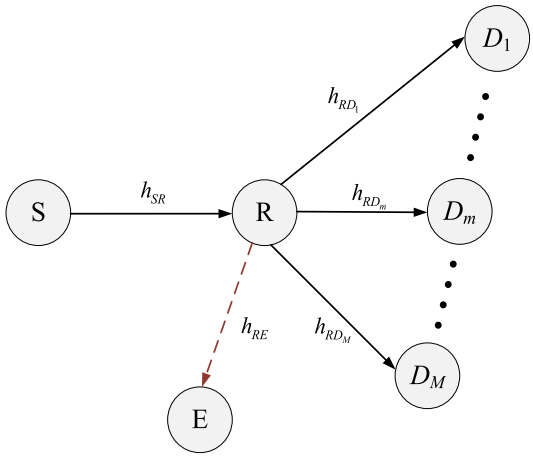

FIGURE 1. C-NOMA system model with eavesdropper.

To the best of our knowledge, the above contributions have not been reported in the open literature.

The remainder of this paper is organized as follows: Section II describes the considered system and channel models, whereas Section III is devoted to the exact and asymptotic analysis of the OP and IP of the considered setup. Section IV provides the respective numerical results and discussions, while closing remarks are given in Section V.

II. SYSTEM MODEL

In this section, we consider a downlink cooperative NOMA (C-NOMA) system with an eavesdropper (E), shown in Fig. 1, where M users (D_m, $m = 1, \ldots, M$) are served by a base station (S) via an AF relay (R) at the same time and frequency, but with different power levels. Without loss of generality, we assume that there is no direct link between S and D_m, which can be justified by the presence of large objects and heavy shadowing conditions encountered between the source and destinations [11]. Furthermore, we assume that E is in the range of the relay (R) only, which can wiretap the signals from R. Here, we model h_{SR}, h_{RD_m}, and h_{RE}, which, respectively, represent the Rayleigh fading gains of the $S \to R, R \to D_m$, and $R \to E$ links, as complex Gaussian random variables with zero mean and variance λ_{SR}, λ_{RD} and λ_{RE}, respectively. This can be considered as the worst-case scenario for mmWave channels [1].

A. SUPERPOSITION CODING

The basic principle underlying NOMA is to allow a certain level of interference from adjacent users by multiplexing different users in the power domain (PD). It is worth noting that power domain multiplexing can be realized by applying superposition coding at the TX, and SIC at the RX. To this end, the base station divides its transmission power among the users, whereas at D_m, multi-user detection is realized by SIC. One of the key challenges is how to allocate the power among NOMA users. In this respect, a common power allocation strategy is the fixed power allocation, where the power ratios

are fixed and ordered according to the users' channel gains. This scenario constitutes the opposite notion of the well-known *water-filling* strategy, since more power is allocated to users with poorer channel conditions. Thus, assuming an ideal RF front end, for $|h_{RD_1}|^2 \leq |h_{RD_2}|^2 \leq ... \leq |h_{RD_M}|^2$, the transmitted signal at S is given by

$$x_S = \sum_{i=1}^{M} \sqrt{P_i} s_i, \tag{1}$$

where $P_i = a_i E_s$ and s_i denote the power and information symbol of the i^{th} sorted user, respectively. Also, E_s is the transmitted power at S, a_i is the i^{th} user's power allocation factor satisfying $a_1 > ... > a_M$ and $\sum_{i=1}^{M} a_i = 1$ [42]. Based on this, the transmission is carried out in two phases: during phase 1, S sends the downlink NOMA signal in (1) to the relay R, and during phase 2, R broadcasts the received signal to the destination nodes, which are also wiretapped by E. To this effect, the received signal at the m^{th} sorted user D_m is given by

$$y_{D_m} = h_{RD_m} G \left(h_{SR} \sum_{i=1}^{M} \sqrt{P_i} s_i + n_R \right) + n_{D_m}, \tag{2}$$

where G is the amplifying coefficient, whereas n_R and n_{D_m} denote the zero mean and variance σ_R^2 and σ_m^2 circularly symmetric complex additive white Gaussian noise (AWGN) at the relay and the m^{th} user, respectively.

B. RESIDUAL HARDWARE IMPAIRMENT

Taking into account the RHI present at the nodes, the received signal at R is represented as [43]

$$y_R = h_{SR} \left(\sum_{i=1}^{M} \sqrt{a_i E_s} s_i + \mu_S \right) + \mu_R + n_R, \tag{3}$$

where μ denotes the distortion noise from RHI and the subscripts S and R denote the source and relay nodes, respectively. Moreover, $\mu_S \sim \mathcal{CN}(0, \rho_S^{t\,2} E_s)$, where ρ_S^t specifies the severity of the TX RHI at the source, whereas $\mu_R \sim \mathcal{CN}\left(0, \rho_R^{r\,2} E_s |h_{SR}|^2\right)$ represents the distortion noise from RX RHI at R. As a result, the distortions from transceiver RHI can be regarded as an additional noise source, yielding

$$y_R = h_{SR} \left(\sum_{i=1}^{M} \sqrt{a_i E_s} s_i + \mu_{SR} \right) + n_R, \tag{4}$$

where $\mu_{SR} \sim \mathcal{CN}(0, \rho_{SR}^2 E_s)$ is the aggregate level of RHI in the link between S and R, and $\rho_{SR}^2 = \rho_S^{t\,2} + \rho_R^{r\,2}$.

Likewise, during phase 2, R amplifies and broadcasts the received signal to the users D_m, where the amplifying coefficient G is given by

$$G = \sqrt{\frac{E_R}{\left(1 + \rho_{SR}^2 E_s |h_{SR}|^2\right) + \sigma_R^2}}, \tag{5}$$

where E_R denotes the transmitted power. Hence, taking into account the RHI at R and D_m, the received signal at D_m can be expressed as

$$y_{D_m} = h_{RD_m} G h_{SR} \left(\sum_{i=1}^{M} \sqrt{a_i E_s} x_i + \mu_{SR} \right) + h_{RD_m} G \left(n_R + \mu_{RD_m} \right) + n_{D_m}, \tag{6}$$

where, $\mu_{RD_m} \sim \mathcal{CN}(0, \rho_{RD_m}^2 E_R)$ is the aggregate level of RHI in the links between R and D_m, and $\rho_{RD_m}^2 = \left(\rho_R^t\right)^2 + \left(\rho_{D_m}^r\right)^2$. The received signal at E in phase 2 is written as:

$$y_E = h_{RE} G \left[h_{SR} \left(\sum_{i=1}^{M} \sqrt{a_i E_s} x_i + \mu_{SR} \right) + n_R + \mu_{RE} \right] + n_E, \tag{7}$$

where n_E is the AWGN at E, $\mu_{RE} \sim \mathcal{CN}(0, \rho_{RE}^2 E_R)$ and $\rho_{RE}^2 = \rho_R^{t\,2} + \rho_E^{r\,2}$ is the aggregate level of RHI between R and E. Moreover, $\rho_R^{t\,2}$ and $\rho_E^{r\,2}$ denote the residual impairment factors at R and E, respectively.[1]

C. SUCCESSIVE INTERFERENCE CANCELLATION

At the users' receivers, SIC is used to realize multi-user detection (MUD) and mitigate interference [3]. Effectively, SIC first decodes users with the higher transmission power and then subtracts them from its received signal while treating all the other users' signals as noise. In particular, user D_k ($k = 1, 2..., M$) first detects the weaker users' signals D_j ($j < k$) and then subtracts them from the received signal. Next, it detects its own signal by treating the stronger users' signals D_l ($l > k$) as noise. Likewise, at the eavesdropper's side, considering the availability of the CSI, the SIC process is also carried out at E. Therefore, assuming perfect interference cancellation, the effective signal for user D_k to decode its own message is given as

$$y_{D_k} = h_{RD_k} G h_{SR} \left(\sum_{i=k}^{M} \sqrt{a_i E_s} x_i + \mu_{SR} \right) + h_{RD_k} G \left(n_R + \mu_{RD_k} \right) + n_{D_k}. \tag{8}$$

[1]For mathematical tractability, hereafter, we assume that the main link noise variance is $\sigma_R^2 = \sigma_m^2 = \sigma^2$, whereas in the wiretap link, the noise variance is σ_e^2.

$$\gamma_{RE}^k = \frac{a_k G^2 E_s |h_{SR}|^2 |h_{RE}|^2}{G^2 |h_{RE}|^2 \left(E_s |h_{SR}|^2 \left(\sum_{j=k+1}^{M} a_j + \rho_{SR}^2 \right) + \sigma^2 \right) + E_R \rho_{RE}^2 |h_{RE}|^2 + \sigma_e^2} \tag{9}$$

III. PERFORMANCE ANALYSIS

Based on the considered C-NOMA downlink network in the presence of an eavesdropper, in this section we determine the outage probability (OP) and intercept probability (IP) performance, which accurately characterize the security and reliability of a wireless communication system [44].

A. INTERCEPT PERFORMANCE

The eavesdropper successfully intercepts the k^{th} legitimate user's signal only if D_k's signal is correctly decoded. It is recalled here that according to the principle of NOMA, users with poor channel quality are allocated more transmission power. Also, we assume perfect cancellation, thus when D_k's signal is wiretapped, E is a able to successfully eliminates the high power users' signals D_j using SIC ($j < k$), whereas the signals of the low power users D_l ($M \geq l > k$) are treated as noise. Based on this and with the aid of (7), the achieved signal to interference plus distortion and noise ratio (SIDNR) of E for decoding D_k's message can be determined using (9), as shown at the bottom of the previous page. Meanwhile, the corresponding data rate achieved at E, when D_k's message is wiretapped, is expressed as follows:

$$C_E^k = \frac{1}{2}\log_2\left(1+\gamma_{RE}^k\right). \tag{10}$$

User D_k will be intercepted if E can successfully wiretap D_k's signal, i.e. $C_E^k \geq R_k$, where R_k denotes user D_k's target rate. Thus, the IP of D_k by E is given by

$$P_{int}^k = \Pr\left(C_E^k \geq R_k\right). \tag{11}$$

Substituting (10) in (11), the IP can be expressed as follows:

$$P_{int}^k = \Pr\left(\gamma_{RE}^k \geq \theta_k\right), \tag{12}$$

where, $\theta_k = 2^{2R_k} - 1$. Moreover, and given that

$$e_0 = \rho_{SR}^2 + \rho_{RE}^2 + \rho_{RE}^2\rho_{SR}^2, \tag{13}$$

$$\Delta_E = \frac{E_s E_R \left|h_{SR}\right|^2 \left|h_{RE}\right|^2}{e_1 E_s \left|h_{SR}\right|^2 + e_2 E_R \left|h_{RE}\right|^2 + \sigma_e^2\sigma^2}, \tag{14}$$

$$e_1 = (1+\rho_{SR}^2)\sigma_e^2, \tag{15}$$

and

$$e_2 = (1+\rho_{RE}^2)\sigma^2. \tag{16}$$

Substituting (9) in (12), yields

$$P_{int}^k = \Pr\left(\frac{a_k\Delta_E}{\left(\sum_{j=k+1}^{M} a_j + e_0\right)\Delta_E + 1} \geq \theta_k\right). \tag{17}$$

Moreover, taking

$$\delta_k = \left(\frac{\alpha_k}{\theta_k} - \left(\sum_{j=k+1}^{M}\alpha_j + e_0\right)\right)^{-1}, \tag{18}$$

which holds for $1 \leq k \leq M-1$, and

$$\delta_M = \left(\frac{\alpha_M}{\theta_M} - e_0\right)^{-1}, \tag{19}$$

For the k^{th} user's message, the intercept probability between R and E can be formulated as in (20), as shown at the bottom of this page . By also recalling that $|h_{SR}|^2$ and $|h_{RE}|^2$ follow Rayleigh distributions for which the probability density function (PDF) is given by

$$f_{|h|^2}(x) = \frac{1}{\lambda}e^{-\frac{x}{\lambda}}, \tag{21}$$

$$\begin{aligned} P_{int}^k &= \Pr\left(\Delta_E \geq \delta_k\right) \\ &= 1 - \Pr\left(E_s\left(E_R\left|h_{RE}\right|^2 - e_1\delta_k\right)\left|h_{SR}\right|^2 \leq \left(e_2E_R\left|h_{RE}\right|^2 + \sigma^2\sigma_e^2\right)\delta_k\right) \\ &= 1 - \int_0^{\frac{e_1\delta_k}{E_R}} f_{|h_{RE}|^2}(v)dv - \int_{\frac{e_1\delta_k}{E_R}}^{\infty} f_{|h_{RE}|^2}(v)\int_0^{\frac{\left(\sigma^2\sigma_e^2+e_2E_Rv\right)\delta_k}{E_s(E_Rv-e_1\delta_k)}} f_{|h_{SR}|^2}(x)dxdv \end{aligned} \tag{20}$$

$$\begin{aligned} P_{int}^k &= \frac{1}{\lambda_{RE}}e^{-\left(\frac{e_1}{E_R\lambda_{RE}}+\frac{e_2}{E_s\lambda_{SR}}\right)\delta_k}\int_0^{\infty} e^{-\frac{\xi}{\lambda_{RE}}-\frac{\left(\sigma^2\sigma_e^2+e_1e_2\delta_k\right)\delta_k}{E_sE_R\lambda_{SE}\xi}}d\xi \\ &= \frac{2}{\lambda_{RE}}e^{-\left(\frac{e_1}{E_R\lambda_{RE}}+\frac{e_2}{E_s\lambda_{SR}}\right)\delta_k}\left(\frac{\lambda_{RE}\left(\sigma^2\sigma_e^2+e_1e_2\delta_k\right)\delta_k}{\lambda_{SR}E_RE_s}\right)^{\frac{1}{2}}K_1\left(2\sqrt{\frac{\left(\sigma^2\sigma_e^2+e_1e_2\delta_k\right)\delta_k}{\lambda_{RE}\lambda_{SR}E_RE_s}}\right) \end{aligned} \tag{22}$$

$$\gamma_{k\to m} = \frac{a_kG^2E_s\left|h_{SR}\right|^2\left|h_{RD}\right|^2}{G^2\left|h_{RD}\right|^2\left(E_s\left|h_{SR}\right|^2\left(\sum_{j=k+1}^{M}a_j + \rho_{SR}^2\right)+\sigma^2\right) + E_R\rho_{RD}^2\left|h_{RD}\right|^2 + \sigma^2} \tag{23}$$

where $\lambda = \mathbb{E}[|h|^2]$ is the corresponding channel variance, taking $\xi = v - \frac{e_1\delta_k}{E_R}$, and using [45, eq. (3.471.9)], the IP is obtained in (22), as shown at the bottom of the previous page.

B. OUTAGE PERFORMANCE

It is recalled that the outage probability can be defined as the probability that the symbol error rate is greater than a certain required quality of service and it can be computed as the probability that the SNR falls below a corresponding threshold which depends on the detection technique, the modulation order, and the encountered fading conditions [46]. According to the principle of NOMA, D_m decodes and cancels the interference from the users allocated more power than itself before decoding its own message. Therefore, D_m should first detect the signals from D_j ($j < m$) before decoding its own signal. Hence, the SIDNR of D_m when decoding D_k's message ($k \leq m$) given in (23), as shown at the bottom of the previous page and the corresponding achievable data rate is evaluated as

$$R_{k\to m} = \frac{1}{2}\log_2(1+\gamma_{k\to m}). \tag{24}$$

Based on the principle of NOMA, an outage event occurs at the m^{th} user if it fails to decode its own signal or the signal of any user in the SIC. Therefore, the m^{th} user's OP is evaluated as

$$P_{out}^m = 1 - P_r(A_{m,1}\cap\cdots\cap A_{m,m}), \tag{25}$$

where $A_{m,k}$ denotes an event in which D_m can correctly decode the k^{th} user's signal and is evaluated as

$$A_{m,k} \triangleq \{R_{k\to m} > R_k\} = \left\{\frac{1}{2}\log_2\left(1+\frac{a_k\Upsilon_{D_m}}{\left(\sum_{j=k+1}^{M} a_j+\rho_0\right)\Upsilon_{D_m}+1}\right) > R_k\right\}, \tag{26}$$

where

$$\rho_0 = \rho_{SR}^2 + \rho_{RD_m}^2 + \rho_{SR}^2\rho_{RD_m}^2, \tag{27}$$

$$\Upsilon_{D_m} = \frac{E_sE_R\,|h_{SR}|^2\,|h_{RD_m}|^2}{\rho_1E_s\,|h_{SR}|^2 + \rho_2E_R\,|h_{RD_m}|^2 + \sigma^4}, \tag{28}$$

$$\rho_1 = (1+\rho_{SR}^2)\sigma^2, \tag{29}$$

and

$$\rho_2 = (1+\rho_{RD_m}^2)\sigma^2. \tag{30}$$

Furthermore, taking

$$\omega_k = \left(\frac{a_k}{2^{2R_k}-1} - \left(\sum_{j=k+1}^{M} a_j+\rho_0\right)\right)^{-1}, \quad 1\leq m\leq M-1 \tag{31}$$

$$\omega_M = \left(\frac{a_M}{2^{2R_k}-1} - \rho_0\right)^{-1}, \tag{32}$$

and

$$\omega_m^* = \max(\omega_1,\cdots,\omega_m), \quad 1\leq m\leq M \tag{33}$$

and assuming independent and identically distributed (i.i.d.) channels h_{RD_m}, while omitting the subscript m for notational convenience, the OP P_{out}^m is formulated according to (34), as shown at the bottom of this page. In addition, $|h_{RD}|^2$ also follows a Rayleigh distribution with variance λ_{RD}; as a result, the corresponding OP is expressed as

$$P_{out}^m = 1 - \int_{\frac{\rho_1\omega_m^*}{E_R}}^{\infty} f_{|h_{RD}|^2}(y)\, e^{-\frac{(\sigma^4+\rho_2E_Ry)\omega_m^*}{\lambda_{SR}E_s(E_Ry-\rho_1\omega_m^*)}}dy. \tag{35}$$

The PDF and cumulative distribution function (CDF) of the m^{th} ordered variable $|h_{RD}|^2$ are given by [11]

$$f_{|h_{RD}|^2}(y) = \frac{Q_m}{\lambda_{RD}}\sum_{i=0}^{M-m}\binom{M-m}{i}(-1)^i e^{-\frac{y}{\lambda_{RD}}} \times\left(1-e^{-\frac{y}{\lambda_{RD}}}\right)^{m+i-1} \tag{36}$$

and

$$F_{|h_{RD}|^2}(y) = Q_m\sum_{i=0}^{M-m}\frac{(-1)^i\binom{M-m}{i}}{m+i}\left(e^{-\frac{y}{\lambda_{RD}}}\right)^{m+i} \tag{37}$$

respectively, where $Q_m = \frac{M!}{(M-m)!(m-1)!}$. By recalling (36) and after some algebraic manipulations, it follows that

$$P_{out}^m = 1 - \frac{Q_m}{\lambda_{RD}}\sum_{i=0}^{M-m}(-1)^i\binom{M-m}{i}\int_{\frac{\rho_1\omega_m^*}{E_R}}^{\infty} e^{-\frac{y}{\lambda_{RD}}} \times\left(1-e^{-\frac{y}{\lambda_{RD}}}\right)^{m+i-1} e^{-\frac{(\sigma^4+\rho_2E_Ry)\omega_m^*}{\lambda_{SR}E_s(E_Ry-\rho_1\omega_m^*)}}dy, \tag{38}$$

$$\begin{aligned} P_{out}^m &= 1-\Pr(\Upsilon_{D_m}>\omega_m^*)\\ &= \Pr(\Upsilon_{D_m}\leq\omega_m^*)\\ &= \Pr\left\{E_s\left(E_R\,|h_{RD}|^2-\rho_1\omega_m^*\right)|h_{SR}|^2 \leq \left(\rho_2E_R\,|h_{RD}|^2+\sigma^4\right)\omega_m^*\right\}\\ &= \int_0^{\frac{\rho_1\omega_m^*}{E_R}} f_{|h_{RD}|^2}(y)dy + \int_{\frac{\rho_1\omega_m^*}{E_R}}^{\infty} f_{|h_{RD}|^2}(y)\int_0^{\frac{(\sigma^4+\rho_2E_Ry)\omega_m^*}{E_s(E_Ry-\rho_1\omega_m^*)}} f_{|h_{SR}|^2}(x)dxdy \end{aligned} \tag{34}$$

where $\rho_2 = 1+\rho_{RD}^2$. Furthermore, by expanding the binomial and taking $z = y - \frac{\rho_1\omega_m^*}{E_R}$, one obtains

$$P_{out}^m = 1 - \frac{Q_m}{\lambda_{RD}} e^{-\frac{\rho_2\omega_m^*}{\lambda_{SR}E_s}} \sum_{i=0}^{M-m} (-1)^i \binom{M-m}{i} \times \sum_{j=0}^{n+i-1} \binom{m+i-1}{j} (-1)^j e^{-\frac{(j+1)\rho_1\omega_m^*}{E_R\lambda_{RD}}} \times \int_0^\infty e^{-\frac{(j+1)}{\lambda_{RD}}z - \frac{\left(\sigma^4+\rho_1\rho_2\omega_m^*\right)\omega_m^*}{\lambda_{SR}E_sE_Rz}} dz. \quad (39)$$

The integral in (39) can be evaluated with the aid of [45, eq. (3.471.9)], which yields the OP expression in (40), as shown at the bottom of this page.

C. ASYMPTOTIC ANALYSIS

1) INTERCEPT PROBABILITY

Given $E_S = E_R = E$ and taking the MER as $\lambda_{me} = \frac{\lambda_{SR}}{\lambda_{RE}}$, in the high MER regime, the asymptotic intercept probability ais obtained as

$$P_{int}^{k\infty} = \frac{2}{\lambda_{RE}} e^{-\left(e_1+\frac{e_2}{\lambda_{me}}\right)\frac{\delta_k}{E\lambda_{RE}}} \left(\frac{\left(\sigma^2\sigma_e^2 + e_1e_2\delta_k\right)\delta_k}{\lambda_{me}E^2}\right)^{\frac{1}{2}} \times K_1\left(2\sqrt{\frac{\left(\sigma^2\sigma_e^2 + e_1e_2\delta_k\right)\delta_k}{\lambda_{me}\lambda_{RE}^2E^2}}\right) \approx e^{-\left(e_1+\frac{e_2}{\lambda_{me}}\right)\frac{\delta_k}{E\lambda_{RE}}}. \quad (41)$$

2) OUTAGE PROBABILITY

Given $E_s = E_R = E$ and letting $\sigma^2 = 1$, equation (28) at high SNR can be simplified as follows

$$\Upsilon_D = \frac{E\Omega_1\Omega_2}{\rho_1\Omega_1 + \rho_2\Omega_2 + \frac{1}{E}} \approx \frac{E\Omega_1\Omega_2}{\rho_1\Omega_1 + \rho_2\Omega_2} \approx E\min\left(\frac{\Omega_1}{\rho_2}, \frac{\Omega_2}{\rho_1}\right), \quad (42)$$

where $\Omega_1 = |h_{SR}|^2$ and $\Omega_2 = |h_{RD}|^2$. Therefore, in the high SNR regime, it follows that

$$P_{out}^{m\infty} \approx 1 - \Pr\left(\min\left(\frac{\Omega_1}{\rho_2}, \frac{\Omega_2}{\rho_1}\right) > \frac{\omega_m^*}{E}\right) = F_{|h_{SR}|^2}\left(\frac{\rho_2\omega_m^*}{E}\right) + F_{|h_{RD}|^2}\left(\frac{\rho_1\omega_m^*}{E}\right) - F_{|h_{SR}|^2}\left(\frac{\rho_2\omega_m^*}{E}\right) \cdot F_{|h_{RD}|^2}\left(\frac{\rho_1\omega_m^*}{E}\right). \quad (43)$$

Also, $\delta_{m\_SR}^* = \rho_2\omega_m^*/E$ and $\delta_{m\_RD}^* = \rho_1\omega_m^*/E$ become $\delta_{m\_SR}^* \to 0$, and $\delta_{m\_RD}^* \to 0$, whilst as $E \to \infty$, it follows that

$$F_{|h_{SR}|^2}\left(\delta_{m\_SR}^*\right) = 1 - e^{-\delta_{m\_SR}^*} \simeq \frac{\delta_{m\_SR}^*}{\lambda_{SR}} \quad (44)$$

and

$$F_{|h_{RD}|^2}\left(\delta_{m\_RD}^*\right) = Q_m \sum_{i=0}^{M-m} \frac{(-1)^i \binom{M-m}{i}}{m+i} e^{-\frac{(m+1)\delta_{m\_RD}^*}{\lambda_{RD}}} \simeq \frac{Q_m}{m}\left(\frac{\delta_{m\_RD}^*}{\lambda_{RD}}\right)^m. \quad (45)$$

Finally, substituting (44) and (45) in (43) yields the following asymptotic OP expression

$$P_{out}^{m\infty} \approx \frac{\delta_{m\_SR}^*}{\lambda_{SR}} + \frac{Q_m}{m}\left(\frac{\delta_{m\_RD}^*}{\lambda_{RD}}\right)^m \left(1 - \frac{\delta_{m\_SR}^*}{\lambda_{SR}}\right). \quad (46)$$

IV. NUMERICAL AND SIMULATION RESULTS

Considering the C-NOMA approach described above and utilizing the derived analytical expressions and their respective computer simulations, this section quantifies the effect of TX and/or RX RHI on the performance of communication systems based on C-NOMA with an eavesdropper (C-NOMA-E). Assuming Rayleigh fading conditions, we carried out extensive Monte Carlo simulations to investigate the IP and OP performance of C-NOMA-E under RHI effects. Unless otherwise stated, the number of users considered is $M = 3$, and the power allocation coefficients are $a_1 = 1/2$, $a_2 = 1/3$ and $a_3 = 1/6$. The associated target data rates are $R_1 = 0.4$bps/Hz, $R_2 = 0.6$ bps/Hz, $R_3 = 0.7$ bps/Hz, respectively[33]. Also, we assume that all the nodes are impaired by RHI, where $\rho_t = \rho_S^t = \rho_R^t$, $\rho_r = \rho_R^r = \rho_{D_m}^r = \rho_E^r$ and we set $\sigma^2 = \sigma_e^2 = 1$, $\lambda = \lambda_{SR} = \lambda_{RD_m} = 1$, and $\lambda_e = \lambda_{SE} = \lambda_{RE}$. Moreover, for a fair comparison, we assume that the transmitted power level is always fixed. This implies that the transmitted signal is normalized by $1 + \rho_t^2$ for TX RHI, by $1/(1 + \rho_r^2)$ for RX RHI and by $(1 + \rho_t^2)/(1 + \rho_r^2)$ for joint TX/RX RHI. Throughout this section, the numerical results are shown with solid lines, whereas markers are used to illustrate the corresponding computer simulation results. Thus, it is clearly observed that the derived expressions accurately characterize the simulated IP and OP performance in the presence of RHI.

$$P_{out}^m = 1 - 2\frac{Q_m}{\lambda_{RD}} e^{-\frac{\rho_2\omega_m^*}{\lambda_{SR}E_s}} \sum_{i=0}^{M-m} (-1)^i \binom{M-m}{i} \sum_{j=0}^{m+i-1} \binom{m+i-1}{j} (-1)^j \left(\frac{\left(\sigma^4 + \rho_1\rho_2\omega_m^*\right)\omega_m^*\lambda_{RD}}{\lambda_{SR}E_sE_R\,(j+1)}\right)^{\frac{1}{2}} \times e^{-\frac{(j+1)\rho_1\omega_m^*}{E_R\lambda_{RD}}} K_1\left(2\sqrt{\frac{\omega_m^*\left(\sigma^4 + \rho_1\rho_2\omega_m^*\right)(j+1)}{\lambda_{RD}\lambda_{SR}E_sE_R}}\right) \quad (40)$$

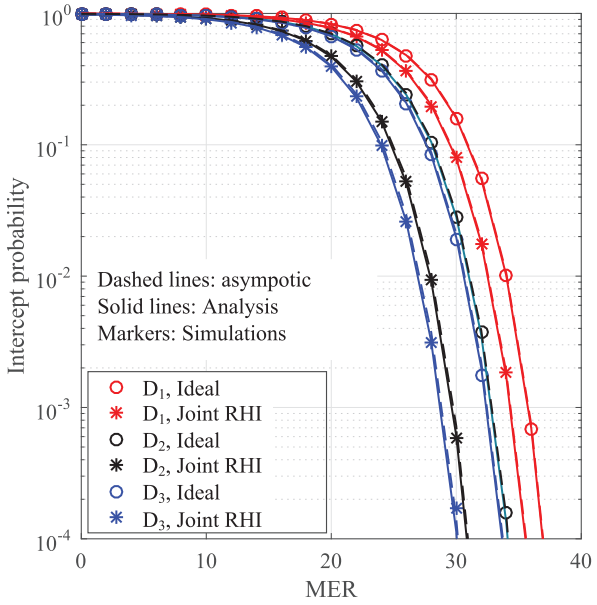

FIGURE 2. IP as a function of MER for a 3 user NOMA system under SIC, SNR=35dB.

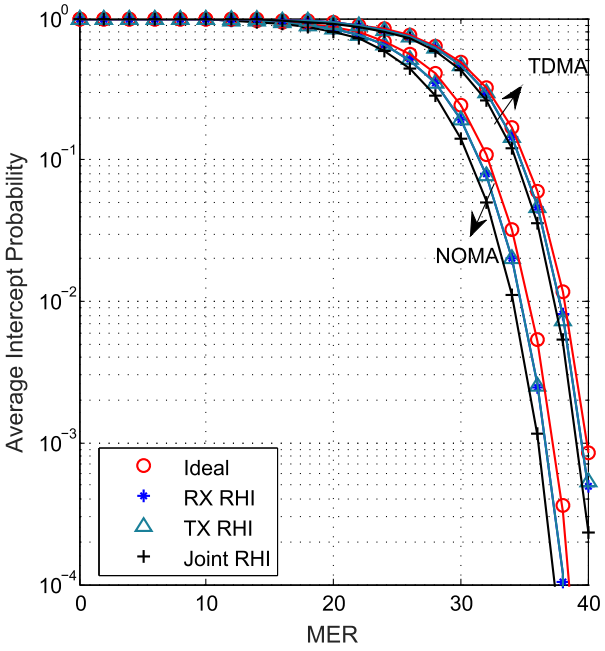

FIGURE 3. Comparison between NOMA and TDMA in terms of the average IP for 3 users, SNR=35dB.

A. EFFECT OF RHI ON THE IP

Fig. 2 illustrates the effects of joint TX/RX RHI on the IP performance of the considered C-NOMA-E system under SIC with three users and one eavesdropper, as a function of the MER. For a transmitted SNR of 35 dB, we evaluated the intercept probability of each NOMA user at E. In this case, RHI may come from the TX and/or RX, where the value of $\rho_{RE} = 0.15$ represents the aggregate level of RHI between R and E. The selected RHI values represent practical values that have been widely used in other relevant analyses. Also, given the assumption of interference cancellation at E, the intercept probability of D_m can be obtained by letting $k = m$ in (22). It is evident that the derived asymptotic expressions provide tight approximations to the exact IP and that RHI reduces the IP probability of the NOMA users. In addition, it is shown that this impairment affects the NOMA users in different ways. For example, in the three-user scenario, RHI has little impact on D_1's IP, whereas the IP of D_2 and D_3 exhibit more significant shifts. Moreover, if we assume that E performs SIC and can therefore eliminate the signals of D_2 and D_3 when D_1 is intercepted, joint TX/RX RHI reduces the highest MER required for E to intercept users D_1, D_2, and D_3 For the three users, the MER declined from 37 dB, 34.1dB, and 33.9 dB to 35.9 dB, 31 dB, and 30 dB, respectively.

The effects of TX RHI only, RX RHI only, and joint TX/RX RHI on the IP performance of a 3 user NOMA system are shown in Fig. 3 for $\rho_r = \rho_t = 0.12$. Fig. 3 also demonstrates the performance of time division multiple access (TDMA) with RHI. For fair comparison, we fix the transmit power to E_s. This implies that for NOMA, E_s is divided between the users during one time slot while for TDMA the transmit power is E_s/M for M time slots. In addition, the target data rate is set to $R = 0.4$ bps/Hz. It is observed that, when considering RHI, NOMA based systems enjoy lower IP compared to TDMA systems. This implies that, in practical scenarios where RHI is inevitable, NOMA is inherently more secure compared to orthogonal multiple access schemes.

Fig. 4 shows the IP of the C-NOMA-E system as a function of the target data rate for a transmitted SNR of 10dB. Here, we assume that the three users have the same target data rate. It is shown again that the decrease in the IP due to RHI depends on many factors, including the NOMA user order, the impairment scenario and the target data rate. For example, for a target data rate of 0.2 bps/Hz, a joint TX/RX RHI $\rho_S^t = \rho_R^t = 0.15$ and $\rho_R^r = \rho_E^r = 0.15$ decreases the IP of D_3's signal by nearly 56%. Meanwhile, when the target data rate is 0.3 bps/Hz, the IP decreases by more than 90%. Moreover, TX and RX RHI influence the IP performance in a similar manner. Given that RHI is an additive impairment, this result is expected in the considered case, where $\rho_{RE} = \sqrt{\left(\rho_R^t\right)^2 + \left(\rho_E^r\right)^2}$.

Fig. 5 demonstrates the average C-NOMA-E IP as a function of the target data rate for different transmitted SNR values, assuming that the target data rate is fixed for all users. It is observed that the impact of the transmitted SNR on the average IP decreases due to TX and/or RX RHI.

Likewise, Fig. 6 shows the IP of a three-user C-NOMA-E as a function of the power allocation coefficient a_1 for RX RHI or TX RHI only, and for joint TX/RX RHI, whilst $a_2 = 2\left(1 - a_1\right)/3$ and $a_3 = \left(1 - a_1\right)/3$. In this context, the effects of RHI on D_1 are insignificant whereas the other users experience a significant decrease in IP due to the encountered RHI. It is also observed that RHI indeed affects the IP. For example, as to D_3, in order to ensure that the IP is lower than 0.01,

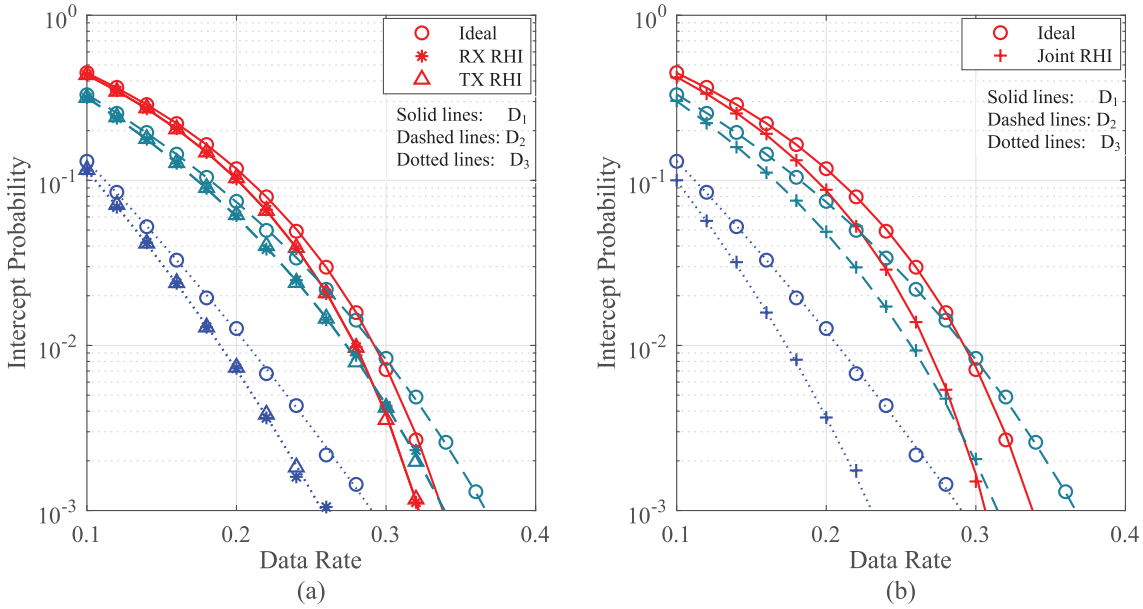

FIGURE 4. IP as a function of data rate for RX RHI only, TX RHI only, and joint TX/RX RHI with SIC, SNR=10dB.

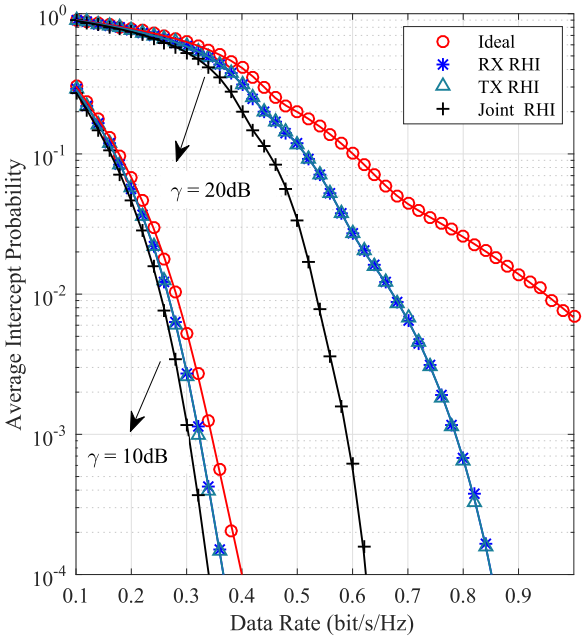

FIGURE 5. Average IP as a function of data rate for RX RHI only, TX RHI only, and joint TX/RX RHI with SIC, MER=10dB.

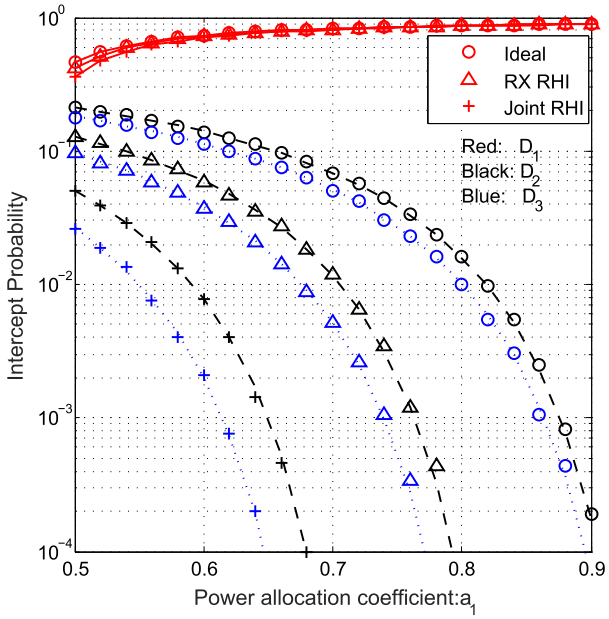

FIGURE 6. IP vs. power allocation coefficient, SNR=20dB, MER=10dB.

a_1 should be larger than 0.55 when there is Joint RHI, while in the ideal case, a_1 should be greater than 0.8.

B. EFFECT OF RHI ON OP

Figs. 7-11 shows the effects of RHI on the OP performance of a three-user C-NOMA-E system as a function of the transmitted SNR. We consider joint TX/RX RHI, and set $\rho_r = \rho_t = 0.14$. The derived asymptotic expressions accurately characterized the exact OP, and it is shown that RHI causes significant degradation of the OP performance for all NOMA users. Moreover, the level of performance degradation depends on the user order. Precisely, from Fig. 7, it is observed that the detrimental effects of RHI appear to affect D_1 less than the other users. Interestingly, under the effects of this impairment, the performance of D_2 and D_3 are degraded to the point where their OP becomes higher than that of D_1. In fact, RHI is an additive impairment, so the severity of the detrimental effects of this impairment depends on several factors, including the power splitting ratio and the user order.

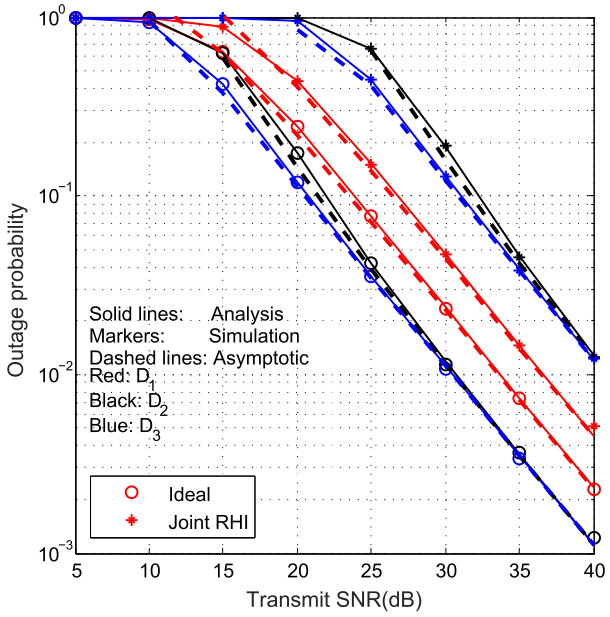

FIGURE 7. OP as a function of transmit SNR for a 3 user NOMA system under joint TX/RX RHI.

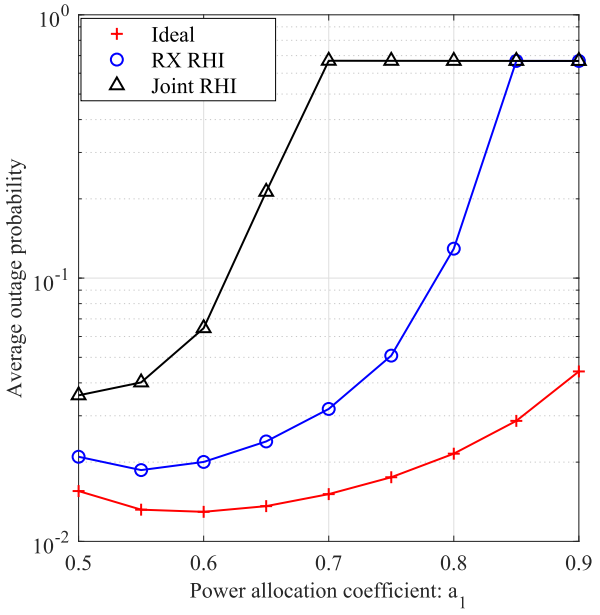

FIGURE 9. Average OP as a function of a_1 for RHI of 0.12.

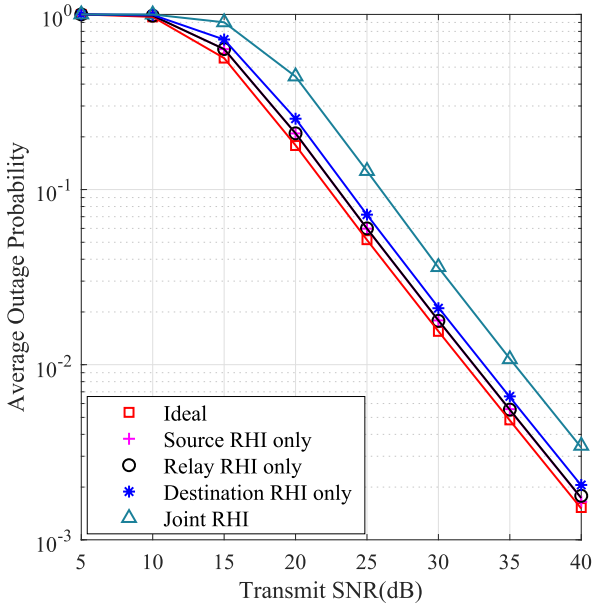

FIGURE 8. Average OP as a function of transmit SNR for RHI of 0.12 at the different nodes.

The effect of RHI at the different nodes is shown in Fig. 8. Interestingly, RHI at the source, relay or destination node only achieves a relatively small increase in the average OP value. In a scenario where RHI occurs solely at the relay node, the performance penalty is of ~ 1.5 dB only. However, joint RHI at all the nodes causes a significant penalty of ~ 4 dB.

Fig. 9, shows the average OP of a three-user C-NOMA-E system as a function of the power allocation ratio a_1 for an SNR of 30 dB with $a_2 = 2\,(1 - a_1)\,/3$ and $a_3 = (1 - a_1)\,/3$. In this scenario, RHI causes a significant increase in the average OP of the system, which greatly depends on the power allocation between the NOMA users, with an OP floor observed in some cases. Moreover, both RX RHI and joint TX/RX RHI affect the optimum power allocation ratio, which minimizes the average OP. This highlights the importance of considering RHI during the analysis and optimization of NOMA systems.

The effect of RHI on the different NOMA users is shown in Fig. 10 for $R_1 = 0.4$ bps/Hz and $R_2 = R_3 = 0.6$ bps/Hz (left) and $R_1 = R_2 = R_3 = 0.4$ bps/Hz (right). By also assuming $a_1 = 0.6$, it is shown that D_1 is quite robust to RHI in both scenarios, even at high RHI levels. The OP of the other two users is increased significantly for average and high levels of RHI. This is due to the power domain multiplexing in NOMA, which allocates less power to higher-order users and renders them more sensitive to noise, interference, and impairments.

Finally, Fig. 11 illustrates the IP against the OP considering a MER of 10 dB and for $R_1 = R_2 = R_3 = 0.4$ bps/Hz. It is shown that for a given IP, the OP of higher-order users (performing SIC) is lower than the OP of lower-order users. This reflects the principle of NOMA where the users are ordered according to their channel gains and higher-order users benefit from better channel conditions. In addition, for a given OP, the presence of RHI generally increases the corresponding IP, and consequently reduces the secure performance. Moreover, it is noted that the observed performance degradation is dependent upon the order of the users, where D_1 is the least affected and experiences almost no performance degradation due to the incurred RHI.

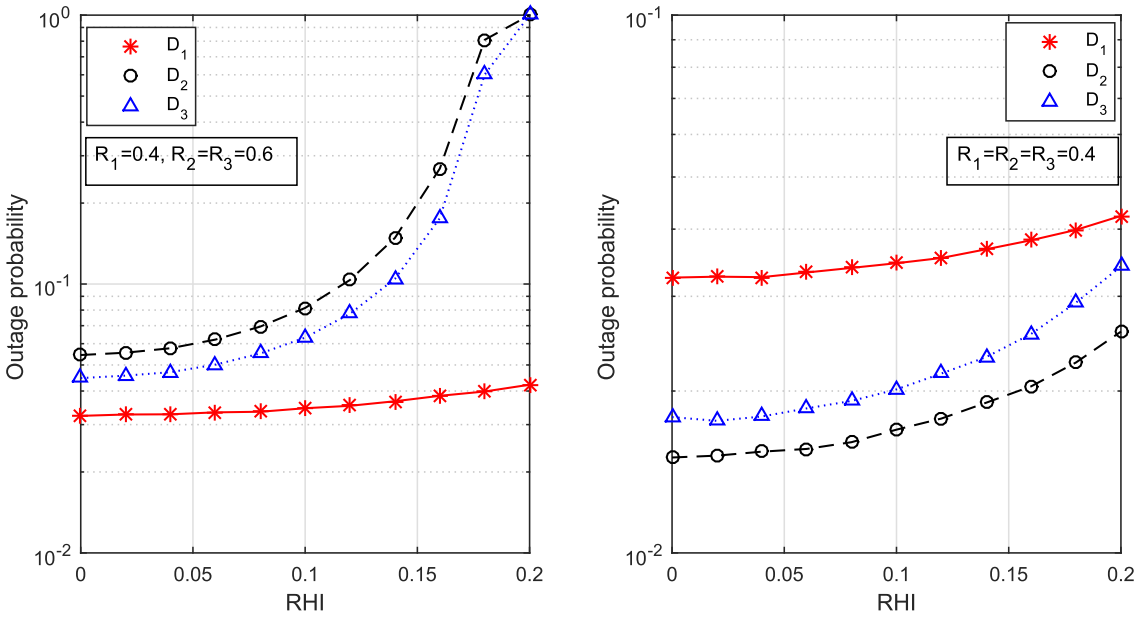

FIGURE 10. OP vs RHI.

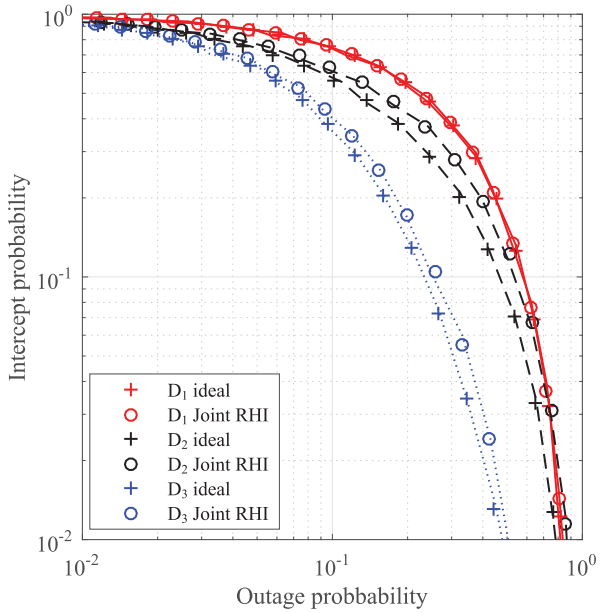

FIGURE 11. IP vs. OP for MER=10dB, $R_1 = R_2 = R_3 = 0.4$bps/Hz.

V. CONCLUSION

We investigated the effects of RHI on secure NOMA-based AF cooperative systems under Rayleigh fading conditions. This was realized by first deriving closed-form expressions for the IP and OP measures of the considered system under RHI. The asymptotic diversity order of the legitimate users and eavesdropper were also derived and the derived analytical results were extensively corroborated by respective computer simulations. Capitalizing on these results, it was shown that RHI degrades both the legitimate users' and the eavesdropper's performance and that the severity of the performance degradation depends on several factors, including the power allocation ratio, the transmitted SNR, the target rate, and the order of the users. Also, RHI can affect the optimal power allocation ratio among users, which highlights the importance of effective modeling and optimization for the efficient implementation of the NOMA paradigm in the fifth generation wireless networks and beyond. In particular, power allocation optimization among users under RHI in multi eavesdroppers case is an interesting problem to pursue in future works.

ACKNOWLEDGMENT

This article was presented in part at the 22nd International Symposium on Wireless Personal Multimedia Communications (WPMC - 2019).

REFERENCES

[1] D. Maamari, N. Devroye, and D. Tuninetti, "Coverage in mmWave cellular networks with base station co-operation," *IEEE Trans. Wireless Commun.*, vol. 15, no. 4, pp. 2981–2994, Apr. 2016.

[2] S. M. R. Islam, N. Avazov, O. A. Dobre, and K.-S. Kwak, "Power-domain non-orthogonal multiple access (NOMA) in 5G systems: Potentials and challenges," *IEEE Commun. Surveys Tuts.*, vol. 19, no. 2, pp. 721–742, 2nd Quart., 2017.

[3] L. Dai, B. Wang, Y. Yuan, S. Han, C.-L. I, and Z. Wang, "Non-orthogonal multiple access for 5G: Solutions, challenges, opportunities, and future research trends," *IEEE Commun. Mag.*, vol. 53, no. 9, pp. 74–81, Sep. 2015.

[4] X. Yue, Z. Qin, Y. Liu, S. Kang, and Y. Chen, "A unified framework for non-orthogonal multiple access," *IEEE Trans. Commun.*, vol. 66, no. 11, pp. 5346–5359, Nov. 2018.

[5] Z. Ding, M. Peng, and H. V. Poor, "Cooperative non-orthogonal multiple access in 5G systems," *IEEE Commun. Lett.*, vol. 19, no. 8, pp. 1462–1465, Aug. 2015.

[6] J.-B. Kim and I.-H. Lee, "Capacity analysis of cooperative relaying systems using non-orthogonal multiple access," *IEEE Commun. Lett.*, vol. 19, no. 11, pp. 1949–1952, Nov. 2015.

[7] M. F. Kader and S. Y. Shin, "Cooperative relaying using space-time block coded non-orthogonal multiple access," *IEEE Trans. Veh. Technol.*, vol. 66, no. 7, pp. 5894–5903, Jul. 2017.

[8] C. Zhong and Z. Zhang, "Non-orthogonal multiple access with cooperative full-duplex relaying," *IEEE Commun. Lett.*, vol. 20, no. 12, pp. 2478–2481, Dec. 2016.

[9] L. Zhang, J. Liu, M. Xiao, G. Wu, Y.-C. Liang, and S. Li, "Performance analysis and optimization in downlink NOMA systems with cooperative full-duplex relaying," *IEEE J. Sel. Areas Commun.*, vol. 35, no. 10, pp. 2398–2412, Oct. 2017.

[10] Z. Ding, H. Dai, and H. V. Poor, "Relay selection for cooperative NOMA," *IEEE Wireless Commun. Lett.*, vol. 5, no. 4, pp. 416–419, Aug. 2016.

[11] J. Men, J. Ge, and C. Zhang, "Performance analysis of nonorthogonal multiple access for relaying networks over Nakagami-*m* fading channels," *IEEE Trans. Veh. Technol.*, vol. 66, no. 2, pp. 1200–1208, Feb. 2017.

[12] J. Men, J. Ge, and C. Zhang, "Performance analysis for downlink relaying aided non-orthogonal multiple access networks with imperfect CSI over Nakagami-*m* fading," *IEEE Access*, vol. 5, pp. 998–1004, Mar. 2017.

[13] Y. Zou, J. Zhu, X. Wang, and L. Hanzo, "A survey on wireless security: Technical challenges, recent advances, and future trends," *Proc. IEEE*, vol. 104, no. 9, pp. 1727–1765, Sep. 2016.

[14] A. Mukherjee, S. A. A. Fakoorian, J. Huang, and A. L. Swindlehurst, "Principles of physical layer security in multiuser wireless networks: A survey," *IEEE Commun. Surveys Tuts.*, vol. 16, no. 3, pp. 1550–1573, 3rd Quart., 2014.

[15] Y. Zou, B. Champagne, W.-P. Zhu, and L. Hanzo, "Relay-selection improves the security-reliability trade-off in cognitive radio systems," *IEEE Trans. Commun.*, vol. 63, no. 1, pp. 215–228, Jan. 2015.

[16] Y. Zou, X. Wang, W. Shen, and L. Hanzo, "Security versus reliability analysis of opportunistic relaying," *IEEE Trans. Veh. Technol.*, vol. 63, no. 6, pp. 2653–2661, Jul. 2014.

[17] Y. Liu, Z. Qin, M. Elkashlan, Y. Gao, and L. Hanzo, "Enhancing the physical layer security of non-orthogonal multiple access in large-scale networks," *IEEE Trans. Wireless Commun.*, vol. 16, no. 3, pp. 1656–1672, Mar. 2017.

[18] Y. Zhang, H.-M. Wang, Q. Yang, and Z. Ding, "Secrecy sum rate maximization in non-orthogonal multiple access," *IEEE Commun. Lett.*, vol. 20, no. 5, pp. 930–933, May 2016.

[19] B. He, A. Liu, N. Yang, and V. K. N. Lau, "On the design of secure non-orthogonal multiple access systems," *IEEE J. Sel. Areas Commun.*, vol. 35, no. 10, pp. 2196–2206, Oct. 2017.

[20] Y. Li, M. Jiang, Q. Zhang, Q. Li, and J. Qin, "Secure beamforming in downlink MISO non-orthogonal multiple access systems," *IEEE Trans. Veh. Technol.*, vol. 66, no. 8, pp. 7563–7567, Aug. 2017.

[21] Z. Ding, Z. Zhao, M. Peng, and H. V. Poor, "On the spectral efficiency and security enhancements of NOMA assisted multicast-unicast streaming," *IEEE Trans. Commun.*, vol. 65, no. 7, pp. 3151–3163, Jul. 2017.

[22] H. Lei, J. Zhang, K.-H. Park, P. Xu, I. S. Ansari, G. Pan, B. Alomair, and M.-S. Alouini, "On secure NOMA systems with transmit antenna selection schemes," *IEEE Access*, vol. 5, pp. 17450–17464, 2017.

[23] H. Lei, Z. Yang, K.-H. Park, I. S. Ansari, Y. Guo, G. Pan, and M.-S. Alouini, "Secrecy outage analysis for cooperative NOMA systems with relay selection schemes," *IEEE Trans. Commun.*, vol. 67, no. 9, pp. 6282–6298, Sep. 2019.

[24] J. Chen, L. Yang, and M.-S. Alouini, "Physical layer security for cooperative NOMA systems," *IEEE Trans. Veh. Technol.*, vol. 67, no. 5, pp. 4645–4649, May 2018.

[25] C. Yu, H.-L. Ko, X. Peng, and W. Xie, "Secrecy outage performance analysis for cooperative NOMA over Nakagami-*m* channel," *IEEE Access*, vol. 7, pp. 79866–79876, Jun. 2019.

[26] C. Liu, L. Zhang, M. Xiao, Z. Chen, and S. Li, "Secrecy performance analysis in downlink NOMA systems with cooperative full-duplex relaying," in *Proc. IEEE Int. Conf. Commun. Workshops (ICC Workshops)*, Jul. 2018, pp. 1–6.

[27] M. Abolpour, M. Mirmohseni, and M. R. Aref, "Outage performance in secure cooperative NOMA," in *Proc. Iran Workshop Commun. Inf. Theory (IWCIT)*, Apr. 2019, pp. 1–6.

[28] B. Razavi, *RF Microelectronics*, vol. 1. Upper Saddle River, NJ, USA: Prentice-Hall, 1998.

[29] L. Chen, A. G. Helmy, G. Yue, S. Li, and N. Al-Dhahir, "Performance analysis and compensation of joint TX/RX I/Q imbalance in differential STBC-OFDM," *IEEE Trans. Veh. Technol.*, vol. 66, no. 7, pp. 6184–6200, Jul. 2017.

[30] A.-A. A. Boulogeorgos, P. C. Sofotasios, B. Selim, S. Muhaidat, G. K. Karagiannidis, and M. Valkama, "Effects of RF impairments in communications over cascaded fading channels," *IEEE Trans. Veh. Technol.*, vol. 65, no. 11, pp. 8878–8894, Nov. 2016.

[31] N. Maletic, M. Cabarkapa, N. Neskovic, and D. Budimir, "Hardware impairments impact on fixed-gain AF relaying performance in Nakagami-*m* fading," *Electron. Lett.*, vol. 52, no. 2, pp. 121–122, Jan. 2016.

[32] W. Xie, X. Xia, Y. Xu, K. Xu, and Y. Wang, "Massive MIMO full-duplex relaying with hardware impairments," *J. Commun. Netw.*, vol. 19, no. 4, pp. 351–362, Aug. 2017.

[33] K. Guo, D. Guo, and B. Zhang, "Performance analysis of two-way multi-antenna multi-relay networks with hardware impairments," *IEEE Access*, vol. 5, pp. 15971–15980, 2017.

[34] A. Papazafeiropoulos, S. K. Sharma, S. Chatzinotas, and B. Ottersten, "Ergodic capacity analysis of AF DH MIMO relay systems with residual transceiver hardware impairments: Conventional and large system limits," *IEEE Trans. Veh. Technol.*, vol. 66, no. 8, pp. 7010–7025, Aug. 2017.

[35] K. Guo, B. Zhang, Y. Huang, and D. Guo, "Outage analysis of multi-relay networks with hardware impairments using SECps scheduling scheme in Shadowed-Rician channel," *IEEE Access*, vol. 5, pp. 5113–5120, Mar. 2017.

[36] B. Selim, S. Muhaidat, P. C. Sofotasios, A. Al-Dweik, B. S. Sharif, and T. Stouraitis, "Radio-frequency front-end impairments: Performance degradation in nonorthogonal multiple access communication systems," *IEEE Veh. Technol. Mag.*, vol. 14, no. 1, pp. 89–97, Mar. 2019.

[37] B. Selim, S. Muhaidat, P. C. Sofotasios, B. S. Sharif, T. Stouraitis, G. K. Karagiannidis, and N. Al-Dhahir, "Performance analysis of non-orthogonal multiple access under I/Q imbalance," *IEEE Access*, vol. 6, pp. 18453–18468, 2018.

[38] F. Ding, H. Wang, S. Zhang, and M. Dai, "Impact of residual hardware impairments on non-orthogonal multiple access based amplify-and-forward relaying networks," *IEEE Access*, vol. 6, pp. 15117–15131, 2018.

[39] X. Li, J. Li, Y. Liu, Z. Ding, and A. Nallanathan, "Outage performance of cooperative NOMA networks with hardware impairments," in *Proc. IEEE Global Commun. Conf. (GLOBECOM)*, Dec. 2018, pp. 1–6.

[40] X. Li, J. Li, P. T. Mathiopoulos, D. Zhang, L. Li, and J. Jin, "Joint impact of hardware impairments and imperfect CSI on cooperative SWIPT NOMA multi-relaying systems," in *Proc. IEEE/CIC Int. Conf. Commun. China (ICCC)*, Aug. 2018, pp. 95–99.

[41] X. Li, J. Li, and L. Li, "Performance analysis of impaired SWIPT NOMA relaying networks over imperfect weibull channels," *IEEE Syst. J.*, to be published.

[42] Z. Yang, Z. Ding, P. Fan, and G. K. Karagiannidis, "On the performance of non-orthogonal multiple access systems with partial channel information," *IEEE Trans. Commun.*, vol. 64, no. 2, pp. 654–667, Feb. 2016.

[43] E. Björnson, A. Papadogiannis, M. Matthaiou, and M. Debbah, "On the impact of transceiver impairments on AF relaying," in *Proc. IEEE Int. Conf. Acoust., Speech Signal Process.*, May 2013, pp. 4948–4952.

[44] J. Zhu, Y. Zou, B. Champagne, W.-P. Zhu, and L. Hanzo, "Security-reliability tradeoff analysis of multirelay-aided decode-and-forward cooperation systems," *IEEE Trans. Veh. Technol.*, vol. 65, no. 7, pp. 5825–5831, Jul. 2016.

[45] I. S. Gradshteyn and I. M. Ryzhik, *Table of Integrals, Series, and Products*, 6th ed. New York, NY, USA: Academic, 2000.

[46] S. J. Grant and J. K. Cavers, "Analytical calculation of outage probability for a general cellular mobile radio system," in *Proc. IEEE VTS 50th Veh. Technol. Conf. Gateway 21st Century Commun. Village (VTC-Fall)*, vol. 3, Sep. 1999, pp. 1372–1376.

MEILING LI was born in Ningwu, Shanxi, China, in 1982. She received the M.S. and Ph.D. degrees in signal and information processing from the Beijing University of Posts and Telecommunications, Beijing, in 2007 and 2012, respectively. She is currently an Associate Professor with the School of Electronics Information Engineering, Taiyuan University of Science and Technology (TYUST), China. She is also a Visiting Research Scholar at the University of Warwick, U.K. Her research interests include cognitive radio, cooperative communications, non-orthogonal multiple access, and physical layer security technology.

BASSANT SELIM (S'15–M'18) received the master's degree in communication systems from Pierre et Marie Curie (Paris XI) University, Paris, France, in 2011, and the Ph.D. degree from Khalifa University, Abu Dhabi, UAE, in 2017. She is currently a Postdoctoral Fellow at the École de Technologie Supérieure, Montreal, Canada. Her research interests include wireless communications, radio-frequency impairments, non-orthogonal multiple access, the IoT, and machine learning.

SAMI MUHAIDAT (S'01–M'07–SM'11) received the Ph.D. degree in electrical and computer engineering from the University of Waterloo, Waterloo, ON, Canada, in 2006. From 2007 to 2008, he was an NSERC Postdoctoral Fellow at the Department of Electrical and Computer Engineering, University of Toronto, Canada. From 2008 to 2012, he was an Assistant Professor with the School of Engineering Science, Simon Fraser University, BC, Canada. He is currently a Professor with Khalifa University. His research focuses on wireless communications, optical communications, the IoT with emphasis on battery-less devices, and machine learning. He is also a member of the Mohammed Bin Rashid Academy of Scientists. He is currently an Area Editor for the IEEE TRANSACTIONS ON COMMUNICATIONS. He has served as a Senior Editor for the IEEE COMMUNICATIONS LETTERS, an Editor for the IEEE TRANSACTIONS ON COMMUNICATIONS, and an Associate Editor for the IEEE TRANSACTIONS ON VEHICULAR TECHNOLOGY.

PASCHALIS C. SOFOTASIOS (S'07–M'12–SM'16) was born in Volos, Greece, in 1978. He received the M.Eng. degree from Newcastle University, U.K., in 2004, the M.Sc. degree from the University of Surrey, U.K., in 2006, and the Ph.D. degree from the University of Leeds, U.K., in 2011. His M.Sc. studies were funded by a scholarship from UK-EPSRC and his Ph.D. studies were sponsored by the UK-EPSRC and Pace plc. He has held academic positions at the University of Leeds, U.K., University of California at Los Angeles, Los Angeles, CA, USA, Tampere University of Technology, Finland, the Aristotle University of Thessaloniki, Greece, and the Khalifa University of Science and Technology, UAE, where he is currently an Assistant Professor. His research interests include broad areas of digital and optical wireless communications, including topics on pure mathematics and statistics. He has been a member and the Co-Chair of the Technical Program Committee of numerous IEEE conferences. He received an Exemplary Reviewer Award from the IEEE Communications Letters, in 2012, and from the IEEE TRANSACTIONS ON COMMUNICATIONS, in 2015 and 2016, respectively. He was a co-recipient of the Best Paper Award at ICUFN'13. He serves as a regular reviewer for several international journals. He currently serves as an Editor for the IEEE COMMUNICATIONS LETTERS.

MEHRDAD DIANATI is currently a Professor of autonomous and connected vehicles with the Warwick Manufacturing Group (WMG), University of Warwick, as well as a Visiting Professor with the 5G Innovation Centre (5GIC), University of Surrey, where he was previously a Professor. He has been involved in a number of national and international projects as the Project Leader and Work-Package Leader in recent years. Prior to his academic endeavour, he has worked in the industry for more than nine years as Senior Software/Hardware Developer and the Director of R&D. He frequently provides voluntary services to the research community in various editorial roles; for example, he has served as an Associate Editor for the IEEE TRANSACTIONS ON VEHICULAR TECHNOLOGY, the *IET Communications*, and the *Journal of Wireless Communications and Mobile (Wiley)*.

PAUL D. YOO is currently with the CSIS within Birkbeck College, University of London. Prior to this, he has held academic/research posts with the Cranfield (Defence Academy of the UK), Sydney (USyd), and South Korea (KAIST). He has amassed more than 60 prestigious journal and conference publications, has been awarded more than 2.3 million US dollars in project funding, and a number of prestigious international and national awards for his work in advanced data analytics, machine learning, and secure systems research, notably the IEEE Outstanding Leadership Award, the Capital Markets CRC Award, the Emirates Foundation Research Award, and the ICT Fund Award. Most recently, he received the prestigious Samsung Award for research to protect the IoT devices. He also serves as an Editor of IEEE COMML and the *Journal of Big Data Research* (Elsevier). He is affiliated with the University of Sydney and the Korea Advanced Institute of Science and Technology (KAIST) as a Visiting Professor.

JIE LIANG (S'99–M'04–SM'11) received the B.E. and M.E. degrees from Xi'an Jiaotong University, China, the M.E. degree from National University of Singapore (NUS), and the Ph.D. degree from the Johns Hopkins University, Baltimore, MA, USA, in 1992, 1995, 1998, and 2003, respectively. Since May 2004, he has been with the School of Engineering Science, Simon Fraser University, Canada, where he is currently a Professor. In 2012, he visited the University of Erlangen-Nuremberg, Germany, as an Alexander von Humboldt Research Fellow. From 2003 to 2004, he worked at the Video Codec Group, Microsoft Digital Media Division. From 1997 to 1999, he was with Hewlett-Packard Singapore and the Center for Wireless Communications, NUS. His research interests include image and video coding, multimedia communications, sparse signal processing, computer vision, and machine learning. He received the 2014 IEEE TCSVT Best Associate Editor Award, the 2014 SFU Dean of Graduate Studies Award for Excellence in Leadership, and the 2015 Canada NSERC Discovery Accelerator Supplements (DAS) Award. He has served as an Associate Editor for the IEEE TRANSACTIONS ON IMAGE PROCESSING, the IEEE TRANSACTIONS ON CIRCUITS AND SYSTEMS FOR VIDEO TECHNOLOGY (TCSVT), the IEEE SIGNAL PROCESSING LETTERS, the *Signal Processing: Image Communication*, and the *EURASIP Journal on Image and Video Processing*.

ANHONG WANG received the Ph.D. degree in multimedia image processing from Beijing Jiaotong University, Beijing, in 2009. She is currently a Professor with the School of Electronics Information Engineering, Taiyuan University of Science and Technology (TYUST), China. Her research interests include image video coding and transmission, compressed sensing, and secret image sharing.